Journal of Magnetic Resonance **142,** 393–396 (2000)
doi:10.1006/jmre.1999.1985, available online at http://www.idealibrary.com on IDEAL®

Direct Refinement against Proton–Proton Dipolar Couplings in NMR Structure Determination of Macromolecules

Nico Tjandra,* John Marquardt,† and G. Marius Clore†

*Laboratory of Biophysical Chemistry, Building 3, National Heart, Lung, and Blood Institute, National Institutes of Health, Bethesda, Maryland 20892-0320; and †Laboratory of Chemical Physics, Building 5, National Institute of Diabetes and Digestive and Kidney Diseases, National Institutes of Health, Bethesda, Maryland 20892-0510

Received October 8, 1999; revised November 17, 1999

The computational tools necessary for making use of ^{1}H–^{1}H dipolar couplings in macromolecular structure refinement are presented. Potentials are described for direct refinement against ^{1}H–^{1}H dipolar couplings of known sign as well as of unknown sign. In addition, a multiple potential is developed for prochiral protons whose stereospecific assignments are unknown. The utility of direct ^{1}H–^{1}H dipolar coupling refinement is illustrated using the small protein ubiquitin. It is shown that direct ^{1}H–^{1}H dipolar coupling refinement leads to improvements in the precision, accuracy, and quality of the resulting structures.

It has been amply demonstrated that backbone dipolar couplings provide valuable information concerning long-range order (*1, 2*) and lead to significant improvements in the accuracy and precision of protein structures determined by NMR (*2–10*). Further improvements in accuracy are potentially attainable by including ^{1}H–^{1}H dipolar couplings (*11–13*) in the structure refinement. To date, however, direct refinement against ^{1}H–^{1}H dipolar couplings has not been carried out. This is in part because the problem of refinement against ^{1}H–^{1}H dipolar couplings corresponding to ^{1}H–^{1}H vectors of varying lengths is more complex than refinement against fixed-length dipolar couplings. In this Communication, we set out the computational tools required for direct ^{1}H–^{1}H dipolar coupling refinement, including cases where the sign of the dipolar coupling is unknown and cases where stereospecific assignments have not been made. We illustrate the application of ^{1}H–^{1}H dipolar coupling refinement using the small protein ubiquitin as an example.

Since ^{1}H–^{1}H vectors are of variable length, the magnitude of the alignment tensor cannot be determined by examining the distribution of ^{1}H–^{1}H dipolar couplings (*14*). Thus, for the purposes of structure refinement, the observed dipolar coupling between two protons A and B is most conveniently expressed as

$$D^{AB}(\theta,\phi) = D_a^{NH}\gamma_H\gamma_N^{-1}\langle r_{NH}^{3}\rangle\langle r_{AB}^{-3}\rangle\{(3\cos^2\theta - 1) + 3/2\,R(\sin^2\theta\cos 2\phi)\}, \quad [1]$$

where D_a^{NH} in units of hertz is the axial component of the traceless second-rank diagonal tensor $\mathbf{D}^{NH}$ for fixed-length backbone N–H vectors; R is the rhombicity defined as the ratio of the rhombic to axial components of the tensor $\mathbf{D}^{NH}$; θ is the angle between the A–B interproton vector and the z axis of the tensor; ϕ is the angle which describes the position of the projection of the A–B interproton vector on the $x - y$ plane, relative to the x axis; γ_H and γ_N are the gyromagnetic ratios of ^{1}H and ^{15}N, respectively; r_{NH} is the fixed distance (1.02 Å) of the N–H bond, and r_{AB} is the distance of the AB interproton vector, where the $\langle\,\rangle$ brackets indicate vibrational averaging. D_a^{NH} and R are readily determined experimentally by examining the distribution of measured ^{15}N–^{1}H and, if available, other fixed-length dipolar couplings (*14*).

If the sign of the ^{1}H–^{1}H dipolar coupling is known, then the penalty function, E_{dip}, which is minimized during simulated annealing refinement, is simply given by

$$E_{dip} = k_{dip}[D^{AB}(\text{calc}) - D^{AB}(\text{obs})]^2, \quad [2]$$

where k_{dip} is the force constant, and D^{AB}(calc) and D^{AB}(obs) are the calculated and observed values of the interproton dipolar couplings. In most instances, however, it is not readily feasible to determine the sign of the ^{1}H–^{1}H dipolar coupling, unless an E.COSY-type experiment (with concomitant loss in signal-to-noise and increase in spectral complexity) is recorded (*13*). In such cases the penalty function that is minimized will be given by

$$E_{dip} = k_{dip}(|D^{AB}(\text{calc})| - |D^{AB}(\text{obs})|)^2, \quad [3]$$

where $|D^{AB}(\text{calc})|$ and $|D^{AB}(\text{obs})|$ are the absolute values of the calculated and observed values of the dipolar couplings.

Many of the measured ^{1}H–^{1}H dipolar couplings involve prochiral protons for which stereospecific assignments may not be available. In such cases we define a multiple dipolar potential for prochiral vectors, $E_{multdipo}$, based on the sums and differences of the observed dipolar couplings similar to those described previously for ^3J coupling constant (*15*) and ^{1}H

1090-7807/00

chemical shift (*16*) refinement, which involves four individual potential terms, E_{d1}, E_{d2}, E_{d3}, and E_{d4}, defined as

$$E_{d1} = k_{d1}\{(\delta_{CalcX} + \delta_{CalcY}) - (\delta_{Obs1} + \delta_{Obs2})\}^2$$
$$E_{d2} = k_{d1}(|\delta_{CalcX} - \delta_{CalcY}| - |\delta_{Obs1} - \delta_{Obs2}|)^2$$
$$E_{d3} = k_{d1}k_{d2}(|\delta_{Obs1} - \delta_{Obs2}| - |\delta_{CalcX} - \delta_{CalcY}|)^2$$
$$E_{d4} = k_{d1}k_{d2}\{0.5(\delta_{Obs1} - \delta_{Obs2})^2 - (\delta_{CalcX} - \delta_{CalcY})^2\}, \quad [4]$$

where δ_{Obs1} and δ_{Obs2} are the values (absolute values when the sign is unknown) of the two observed dipolar couplings (in arbitrary order), δ_{CalcX} and δ_{CalcY} are the values (absolute values when the sign is unkown) of the two expected dipolar couplings (in arbitrary order) calculated from the structure, k_{d1} is a force constant, and k_{d2} is a scale factor. The optimal value of k_{d2}, which readily permits the transition from the incorrect to the correct stereospecific assignment, is found empirically to be 0.2. $E_{multidipo}$ is then given by

$$\begin{aligned} E_{multidipo} &= E_{d1} + E_{d2}, \quad \text{if } |\delta_{CalcX} - \delta_{CalcY}| > |\delta_{Obs1} - \delta_{Obs2}| \\ &= E_{d1} + E_{d3}, \quad \text{if } |\delta_{Obs1} - \delta_{Obs2}| \geq |\delta_{CalcX} - \delta_{CalcY}| \\ &\qquad \geq 0.5|\delta_{Obs1} - \delta_{Obs2}| \\ &= E_{d1} + E_{d4}, \quad \text{if } |\delta_{CalcX} - \delta_{CalcY}| \\ &\qquad < 0.5|\delta_{Obs1} - \delta_{Obs2}|. \end{aligned} \quad [5]$$

To test the utility of ^{1}H–^{1}H dipolar coupling refinement, we carried out a series of simulated annealing calculations (*17*) using XPLOR/CNS (*18, 19*) on the small 76-residue protein ubiquitin for which a large number of structurally useful NOEs have been previously assigned ((*20*) and J.M., unpublished data). ^{1}H–^{1}H dipolar couplings were measured from a 3D quantitative *J* H_N–H_α correlation experiment recorded on a sample of uniformly ^{15}N-labeled ubiquitin in a bicelle liquid crystalline medium (5% w/v 3:1 DMPC:DHPC) (*1*). In this particular experiment the differential relaxation rates between the diagonal and cross peaks result in a small underestimate of the dipolar couplings (*21*). However, as has been shown previously (*21*), the fractional error, to a good approximation, is independent of the size of the coupling. Hence, underestimating the value of the ^{1}H–^{1}H dipolar coupling is equivalent to having a slightly smaller effective D_a^{NH}. The percent correction for a molecule in the slow tumbling limit would be of the order of 10–20% of the measured dipolar couplings. A change of this magnitude in the value of D_a^{NH} will not have any significant effect on the calculated structures (*2, 22*). It is also interesting to note that if very high precision ^{1}H–^{1}H dipolar couplings could be measured, a variation in the correction factor could potentially be determined in the presence of a highly accurate known structure. The variation, however, in the correction factor for large molecules is less than 5% (*21*), so that the measured dipolar couplings would have to be measured to a precision of better than 0.5 Hz. With the current data it is clearly impossible to detect such variations.

TABLE 1

Agreement between Observed and Calculated ^{1}H–^{1}H and ^{15}N–^{1}H Dipolar Couplings for the "High-Resolution" NMR Structure (*20*) and the 1.8-Å-Resolution Crystal Structure (*23*)

	High-resolution NMR structure[a]	X-ray structure[b]
RMS deviation from ^{1}H–^{1}H dipolar coupling restraints (Hz)		
All (589)	1.39	1.40
$D_{H_N(i)-H_\alpha(i)}$ (42)	0.82	1.09
$D_{H_N-other}$ (48)	1.42	2.03
Null D_{H_N-H} (499)	1.42	1.36
RMS deviation from $^1D_{NH}$, dipolar couplings (Hz) (53)	1.71	1.59

[a] PDB Accession Code 1D3Z (*20*).
[b] PDB Accession Code 1UBQ (*23*). Protons were added using standard geometry with XPLOR/CNS (*18, 19*).

$H_N(i)$–$H_\alpha(i)$ dipolar couplings were obtained from the difference in $^3J_{HN\alpha}$ couplings measured in isotropic and liquid crystalline media (*1*). The other correlations observed in the 3D quantitative *J* H_N–H_α experiment in the liquid crystalline medium arise solely from dipolar couplings since they have zero *J* coupling values in isotropic medium (*1*). The signs of these ^{1}H–^{1}H dipolar couplings, however, cannot be determined from the 3D quantitative *J* H_N–H_α correlation experiment. ^{1}H–^{15}N dipolar couplings were determined from the difference in $^1J_{H_N}$ couplings obtained in liquid crystalline and isotropic media measured in a coupled ^{1}H–^{15}N correlation spectrum. The experimental data comprise 1537 experimental distance restraints (1485 unique structurally useful NOE-derived interproton distances and 52 distances corresponding to 26 backbone hydrogen bonds), 56 $^3J_{HN\alpha}$ coupling constant restraints, 53 $^1D_{NH}$ dipolar coupling restraints, 42 $D_{H_N(i)-H_\alpha(i)}$ dipolar coupling restraints of known sign, and 48 $D_{H_N-H(other)}$ dipolar coupling restraints of unknown sign. (The latter include interresidue H_N–H_α interactions as well as H_N–side chain interactions). Given knowledge of the noise and the magnitude of the diagonal peak, it is a simple matter to estimate the minimum value for a dipolar coupling that can be observed in the 3D quantitative *J* H_N–H_α experiment. In this particular case this corresponds to about 2 Hz. It is therefore possible to also derive structurally useful restraints from the absence of an observed cross peak in the spectrum recorded in the liquid crystalline medium. On this basis, we also derived a set of 499 so-called "null" (or "negative") ^{1}H–^{1}H dipolar coupling restraints for which no correlations were observed in the 3D quantitative *J* H_N–H_α experiment recorded in the liquid crystalline medium. Since the magnitude of the ^{1}H–^{1}H di-

polar coupling is related to the inverse cube of the corresponding interproton distance, we restricted the null ^{1}H–^{1}H dipolar coupling restraints to vectors which had distances $\leq$5 Å in the structure refined without ^{1}H–^{1}H dipolar couplings. The null ^{1}H–^{1}H dipolar coupling restraints were restricted to a range of 0 $\pm$ 2 Hz by a square-well potential. Harmonic potentials were employed for the $^3J_{\mathrm{HN}\alpha}$, $^1D_{\mathrm{NH}}$, and $D_{\mathrm{H_N}(i)-\mathrm{H}\alpha(i)}$ restraints, while square-well potentials were employed for the NOE-derived interproton distance restraints and remaining ^{1}H–^{1}H dipolar coupling restraints. In the latter case an error range of $\pm$2 Hz was employed. Two sets of calculations were carried out, one with and the other without the inclusion of the ^{1}H–^{1}H dipolar coupling restraints.

TABLE 2
Structural Statistics[a]

	With ^{1}H–^{1}H dipolar couplings[b]	Without ^{1}H–^{1}H dipolar couplings[b]
RMS deviation from ^{1}H–^{1}H dipolar coupling restraints (Hz)		
All (589)	0.79 ± 0.07	2.47 ± 0.19
$D_{\mathrm{H_N}(i)-\mathrm{H}\alpha(i)}$ (42)	0.83 ± 0.07	1.42 ± 0.34
$D_{\mathrm{HN-other}}$ (48)	0.74 ± 0.18	4.26 ± 0.69
Null $D_{\mathrm{H_N-H}}$ (499)	0.44 ± 0.02	2.44 ± 0.25
RMS deviation from $^1D_{\mathrm{NH}}$ dipolar couplings (Hz) (53)[c]	0.54 ± 0.033	0.52 ± 0.04
RMS deviations from interproton distance restraints (Å) (1537)[d]	0.038 ± 0.007	0.033 ± 0.005
RMS deviation from $^3J_{\mathrm{HN}\alpha}$ coupling constants (Hz) (56)	0.87 ± 0.06	0.69 ± 0.10
Lennard–Jones energy (kcal.mol^{-1})[e]	−289 ± 10	−288 ± 13
% Residues in most favored region of Ramachandran plot	82.4 ± 1.5	75.4 ± 4.2
Backbone coordinate precision (Å)	0.43	0.56
Backbone coordinate accuracy (Å)[f]	0.53/0.62	0.61/0.67

[a] The number of restraints are given in parentheses. The force constants employed for the NOE-derived interproton distance restraints, the dipolar couplings, and the $^3J_{\mathrm{HN}\alpha}$ couplings are 30 kcal.mol^{-1}.Å^{-2}, 1 kcal.mol^{-1}.Hz^{-2}, and 1 kcal.mol^{-1}.Hz^{-2}, respectively. The scale factor k_{d2} in Eq. [4] is set to 0.2. The force constant for the quartic van der Waals repulsion term (*17*) used to prevent atoms from coming too close together is set to 4 kcal.mol^{-1}.Å^{-4} with the van der Waals radius scale factor set to 0.8.

[b] Ten simulated annealing structures were calculated for each ensemble.

[c] The values of D_a^{NH} and R are −9.6 Hz and 0.27, respectively, and were determined as described in (*13*).

[d] The interproton distance restraints comprise 340 sequential ($|i - j| = 1$), 267 short-range ($1 < |i - j| \leq 5$), and 588 long-range ($|i - j| > 5$) interresidue restraints and 290 structurally useful intraresidue restraints. In addition, there are 52 distance restraints for 26 backbone hydrogen bonds.

[e] The Lennard–Jones van der Waals energy is calculated with the CHARMM19/20 parameters and is not included in the target function for simulated annealing.

[f] Accuracy for the backbone (N, Cα, C, O atoms) is defined as the rms difference between the mean coordinates of the ensemble of simulated annealing structures and either the "high-resolution" NMR structure (*20*) (first number) or the 1.8-Å-resolution X-ray structure (*23*) (second number). The rmsd is calculated for residues 3–70 since the N- (residues 1–2) and C- (residues 71–76) terminal residues are disordered in solution.

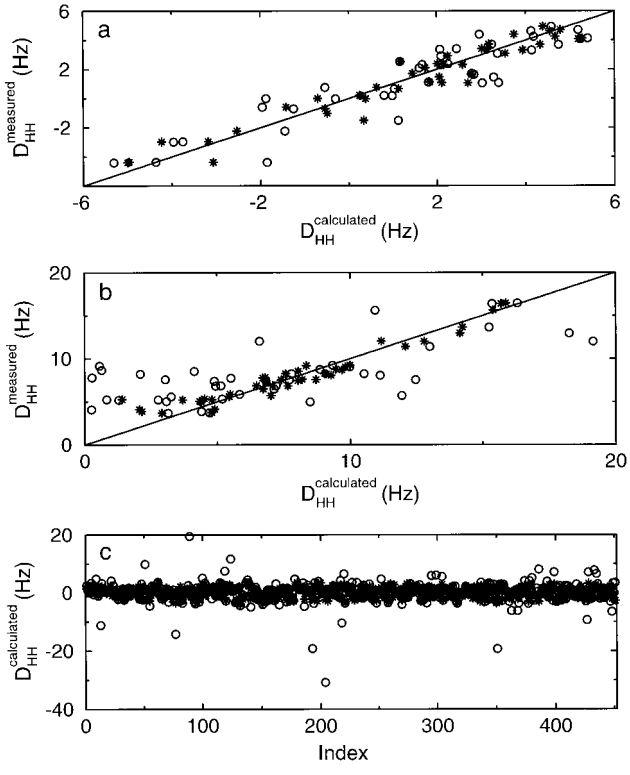

FIG. 1. Agreement between observed and calculated ^{1}H–^{1}H dipolar couplings for ubiquitin with (*) and without (○) refinement against ^{1}H–^{1}H dipolar couplings. (a) $D_{\mathrm{H_N}(i)-\mathrm{H}\alpha(i)}$ couplings whose sign is known; (b) $D_{\mathrm{H_N-H}}$ couplings whose signs are unknown; (c) "null" $D_{\mathrm{H_N-H}}$ dipolar couplings.

The agreement between measured and calculated ^{1}H–^{1}H and $^1D_{\mathrm{NH}}$ dipolar couplings for the X-ray structure (*23*) and the "high-resolution" NMR structure (*20*) is given in Table 1. The high-resolution NMR structure was derived from 2727 (not all unique) NOE-derived interproton distance restraints, 98 torsion angle restraints, and 372 fixed-length dipolar coupling restraints (*20*). It is apparent that the agreement between observed and calculated ^{1}H–^{1}H dipolar couplings is similar for these two structures, suggesting that their coordinate accuracy is comparable. Thus, these two structures serve as useful reference structures for the present set of calculations.

The results of the calculations are summarized in Table 2 and Fig. 1. In the absence of ^{1}H–^{1}H dipolar coupling refinement, the agreement between observed and calculated ^{1}H–^{1}H dipolar couplings is significantly worse than it is for either the X-ray structure (*23*) or the high-resolution NMR structure (*20*). Upon ^{1}H–^{1}H dipolar coupling refinement there is a significant improvement in the agreement between observed and calculated ^{1}H–^{1}H dipolar couplings which is now better than for either the X-ray structure or the high-resolution NMR structure; this includes both backbone–backbone, backbone–side chain, and the so-called null dipolar couplings (Fig. 1 and Table 2). Inclusion of ^{1}H–^{1}H dipolar couplings results in a

backbone atomic rms shift of 0.43 Å in the mean coordinate positions, but does not significantly affect the agreement with the other experimental restraints (interproton distances, $^{3}J_{HN\alpha}$ couplings, and $^{1}D_{NH}$ dipolar couplings), the deviations from idealized covalent geometry, or the quality of the nonbonded contacts (Table 1). Both the precision and the accuracy of the coordinates (the latter measured by reference to both the high-resolution NMR structure (*20*) and the 1.8-Å crystal structure of ubiquitin (*23*)) are slightly increased upon inclusion of the $^{1}H–^{1}H$ dipolar couplings (Table 1). Also slightly improved is the quality of the Ramachandran map (Table 1).

In conclusion, $^{1}H–^{1}H$ dipolar couplings can be readily included in protein structure refinement and do result in an improvement in precision and accuracy without compromising the agreement with other structural restraints or the overall quality of the structure. It should be borne in mind, however, that since $^{1}H–^{1}H$ dipolar couplings exhibit both an angular and a distance dependence, they are conformationally less restrictive than dipolar couplings corresponding to fixed-length bond vectors.

ACKNOWLEDGMENT

We thank Ad Bax for useful discussions.

REFERENCES

1. N. Tjandra and A. Bax, Direct measurement of distances and angles in biomolecules by NMR in a dilute liquid crystalline medium. *Science* **278,** 1111–1114 (1997).
2. N. Tjandra, J. G. Omichinski, A. M. Gronenborn, G. M. Clore, and A. Bax, Use of dipolar $^{1}H–^{15}N$ and $^{1}H–^{13}C$ couplings in the structure determination of magnetically oriented macromolecules in solution. *Nat. Struct. Biol.* **4,** 732–738 (1997).
3. C. A. Bewley, K. R. Gustafson, M. R. Boyd, D. G. Covell, A. Bax, G. M. Clore, and A. M. Gronenborn, Solution structure of cyanovirin-N, a potent HIV-inactivating protein. *Nat. Struct. Biol.* **5,** 571–578 (1998).
4. M. Cai, Y. Huang, R. Zheng, S.-Q. Wei, R. Guirlando, M. S. Lee, R. Craigie, A. M. Gronenborn, and G. M. Clore, Solution structure of the cellular factor BAF responsible for protecting retroviral DNA from autointegration. *Nat. Struct. Biol.* **5,** 903–909 (1998).
5. D. S. Garrett, Y.-J. Seok, A. Peterkofsky, A. M. Gronenborn, and G. M. Clore, Solution structure of the 40,000 Mr phosphoryl transfer complex between the N-terminal domain of enzyme I and HPr. *Nat. Struct. Biol.* **6,** 166–173 (1999).
6. G. M. Clore, M. R. Starich, C. A. Bewley, M. Cai, and J. Kuszewski, Impact of residual dipolar couplings on the accuracy of NMR structures determined from a minimal number of NOE restraints. *J. Am. Chem. Soc.* **121,** 6513–6514 (1999).
7. A. C. Drohat, N. Tjandra, D. M. Baldisseri, and D. Weber, The use of dipolar couplings for determining the solution structure of rat apo-S100B. *Protein Sci.* **8,** 800–809 (1999).
8. J. L. Barber, D. Libutti, D. Levens, and N. Tjandra, High precision solution structure of the C-terminal KH domain of heterogeneous nuclear ribonucleoprotein K, a c-myc transcription factor. *J. Mol. Biol.* **289,** 949–962 (1999).
9. E. de Alba, L. de Vries, M. G. Farquhar, and N. Tjandra, Solution structure of human GAIP (G alpha interacting protein): A regulator of G protein signalling. *J. Mol. Biol.* **292,** 927–939 (1999).
10. G. M. Clore, and D. S. Garrett, R-factor, free R and complete cross-validation for dipolar coupling refinement of NMR structures. *J. Am. Chem. Soc.* **121,** 9008–9012 (1999).
11. M. R. Hansen, M. Rance, and A. Pardi, Observation of long range $^{1}H–^{1}H$ distances in solution by dipolar coupling interactions. *J. Am. Chem. Soc.* **120,** 11210–11211 (1998).
12. M. R. Hansen, L. Mueller, and A. Pardi, Tunable alignement of macromolecules by filamentous phage yields dipolar coupling interactions. *Nat. Struct. Biol.* **5,** 1065–1074.
13. M. Cai, H. Wang, E. T. Olejniczak, R. P. Meadows, A. H. Gunasekera, N. Xu, and S. W. Fesik, Accurate measurement of $H^{N}–H^{\alpha}$ residual dipolar couplings in proteins. *J. Magn. Reson.* **139,** 451–453 (1999).
14. G. M. Clore, A. M. Gronenborn, and A. Bax, A robust method for determining the magnitude of the fully asymmetric alignment tensor of oriented macromolecules in the absence of structural information. *J. Magn. Reson.* **133,** 216–221 (1998).
15. K. L. Constantine, M. S. Friedrichs, L. Mueller, and R. E. Bruccoleri, *J* coupling restraint potentials for nonstereospecifically assigned methylene protons and ensemble-average calculations. *J. Magn. Reson. B* **108,** 176–184 (1995).
16. J. Kuszewski, A. M. Gronenborn, and G. M. Clore, A potential involving multiple proton chemical-shift restraints for nonstereospecifically assigned methyl and methylene protons. *J. Magn. Reson. B* **112,** 79–81 (1996).
17. M. Nilges, A. M. Gronenborn, A. T. Brünger, and G. M. Clore, Determination of three-dimensional structures of proteins by simulated annealingwith interproton distance restraints: Application to crambin, potato carboxypeptidase inhibitor and barley serine proteinase inhibitor 2. *Prot. Eng.* **2,** 27–38 (1988).
18. A. T. Brünger, "X-PLOR: A System for X-Ray Crystallography and NMR," Yale Univ. Press, New Haven, CT (1993).
19. A. T. Brünger, P. D. Adams, G. M. Clore, W. L. Delano, P. Gros, R. W. Grosse-Gunstleve, J.-S. Jiang, J. Kuszewski, M. Nilges, N. S. Pannu, R. J. Read, L. M. Rice, T. Simonson, and G. L. Warren, Crystallography & NMR system: A new software suite for macromolecular structure determination. *Acta Crystallogr.* **D54,** 905–921 (1998).
20. G. Cornilescu, J. L. Marquardt, M. Ottiger, and A. Bax, Validation of protein structure from anisotropic carbonyl chemical shifts in a dilute liquid crystalline phase. *J. Am. Chem. Soc.* **120,** 6836–6837 (1998).
21. G. W. Vuister, and A. Bax, Quantitative J correlation: A new approach for measuring homonuclear three bond $J(H^{N}H\alpha)$ coupling constants in ^{15}N enriched proteins. *J. Am. Chem. Soc.* **115,** 7772–7777 (1993).
22. G. M. Clore, A. M. Gronenborn, and N. Tjandra, Direct structure refinement against residual dipolar couplings in the presence of rhombicity of unknown magntitude. *J. Magn. Reson.* **131,** 159–162 (1998).
23. S. Vijay-Kumar, C. E. Bugg, and W. J. Cook, Structure of ubiquitin at 1.8 Å resolution. *J. Mol. Biol.* **194,** 531–544 (1987).